



Investigating Amorphous Metal Composite Architectures as Spacecraft Shielding*

Marc Davidson¹, Scott Roberts², Gerhard Castro¹, Robert Peter Dillon³, Allison Kunz², Henry Kozachkov², Marios D. Demetriou², William L. Johnson², Steve Nutt¹, Douglas C. Hofmann^{2,3}

1. Department of Chemical Engineering and Materials Science, University of Southern California, Los Angeles, CA 90089, USA
2. Affiliated Keck Laboratory of Engineering, California Institute of Technology, Pasadena, CA 91125, USA. E-mail: dch@jpl.nasa.gov
3. Engineering and Science Directorate, Jet Propulsion Laboratory, California Institute of Technology, Pasadena, CA 91109, USA

Abstract: The threat of micro-meteoroid and orbital debris (MMOD) collisions with spacecraft and satellites has been increasing with the increasing worldwide use of low earth orbit. Providing low-area-density shielding for the mitigation of these high velocity impacts is essential for ensuring successful and cost effective missions. Here, we report results obtained from hypervelocity impact testing on bulk metallic glass (BMG) matrix composites. Their carbide-like hardness, low melting temperatures, ultra-high strength-to-weight ratio and the ability to be processed like polymers are material attributes ideally suited for spacecraft shielding, particularly as an outer wall bumper shield.

* This work was supported by the Strategic University Research Partnership at the Jet Propulsion Laboratory, California Institute of Technology. Graduate student support was provided by the Office of Naval Research under grant no. N00014-07-1-1115, the Education Office of the Jet Propulsion Laboratory, California Institute of Technology, and NASA's Exploration Systems Mission Directorate under contract number NNH10ZTT001N. The authors thank the staff of the NASA Ames Vertical Gun Range for their technical support of this effort, especially D. Holt and C. Cornelison. The authors also thank Eric Christiansen of NASA's Johnson Space Center for supplying the ballistic limit equations program and comments. Supporting Information is available from the Wiley Online Library or from the author

Please cite this article as M Davidson, S Roberts, G Castro, RP Dillon, A Kunz, H Kozachkov, MD Demetriou, WL Johnson, S Nutt, DC Hofmann "**Investigating Amorphous Metal Composite Architectures as Spacecraft Shielding**", Adv Engrg Matls (2012)
DOI<<http://dx.doi.org/10.1002/adem.201200313>>



As human activity has increased in low-earth orbit so has the accumulation of space debris and the corresponding hazard to space vehicles [1–3]. From 1960 to 1996, the number of objects in orbit increased linearly at a rate of approximately 250 objects per year [2]. Since 1996, however, the number of objects in orbit has been increasing exponentially due to a combination of low-cost space technology and a larger number of nations launching spacecraft and satellites. The primary hazard to space vehicles from micrometeoroid and orbital debris (MMOD), comprising fragmentation debris, spacecraft, rocket bodies, and operational debris, is the kinetic energy of these masses traveling at hyper velocities ($5\text{--}15\text{ km s}^{-1}$)[1–6].

Large debris, generally considered to be objects larger than 100 mm in diameter, can be tracked and characterized by ground-based radar for attitude, size, shape, orbital lifetime, ballistic coefficient, and mass [2]. An impact with large debris is catastrophic for most space vehicles and collision avoidance maneuvers have been used in the past by Space Shuttle, satellites, and the International Space Station (ISS) to prevent such an occurrence [3]. Conversely, small debris, projectiles too small to detect and avoid, has already caused damage to operational space systems [2]. To mitigate the risk of loss of function or mission failure from small debris collisions, particularly from 1 to 5 mm diameter particles, spacecraft designers incorporate implicit protection into vehicle architecture, and explicit MMOD shield impact protection concepts[5].

A range of shield concepts, including single metal sheets, complex layers of metals, carbon composites, fabrics, and honeycomb sandwich panels (HSPs), have been studied and implemented into space vehicles to mitigate the risk of MMOD impacts [3–7]. The most common type of shield, developed by Fred Whipple in the 1940s, consists of multiple layers separated by a gap, called a

Please cite this article as M Davidson, S Roberts, G Castro, RP Dillon, A Kunz, H Kozachkov, MD Demetriou, WL Johnson, S Nutt, DC Hofmann “**Investigating Amorphous Metal Composite Architectures as Spacecraft Shielding**”, Adv Engrg Matls (2012)
DOI<<http://dx.doi.org/10.1002/adem.201200313>>



standoff. The front facesheet of the shield is called the “bumper” and the rear facesheet is called the “rear wall.” The bumper breaks up the impacting particle into a spray of melt and vapor that expands while moving through the standoff. Dispersion of the debris cloud over a wider area of the rear wall helps prevent perforation or detached spall. Successful operation of the shield requires the rear wall survive this impulsive loading. The performance of MMOD shields is often estimated using computer simulations and hydrocodes developed from ballistic limit equations (BLEs) obtained via hypervelocity testing. [5–13]. For a given shield configuration, test variables include projectile size, velocity, density, and impact angle. The data obtained from a hypervelocity test program are then used to statistically predict the performance of a shield and establish design parameters. For example, the minimum thickness (t_{Ti} , cm) of a titanium wall to prevent a given amount of damage is given by the empirical BLE [5,7]:

$$t_{Ti} = 5.24d \cdot K \cdot BHN^{-0.25} \left(\frac{\rho_p}{\rho_t} \right)^{0.5} \left(\frac{V \cos \theta}{C_t} \right)^{2/3} \quad (1)$$

where d is the projectile diameter (cm), K the damage parameter for titanium (either 1.8, 2.4, or 3 for perforation, detached spall, or incipient attached spall, respectively), BHN the Brinell hardness of the target, r the density of the projectile (p) and target (t)($g\ cm^{-3}$), C_t the speed of sound in the target ($km\ s^{-1}$), V the projectile velocity ($km\ s^{-1}$), and u is the impact angle from target normal. Thus, a single wall of Ti-15-3-3-3 must be at least 2 mm thick to prevent detached spall from the impact of a 0.8 mm aluminum projectile impacting normal to the plate at a velocity of $6.4\ km\ s^{-1}$. Equation (1) for titanium shields demonstrates that the material properties which have the most effect on ballistic performance are the hardness and density of the shield (and to a lesser extent, the speed of

Please cite this article as M Davidson, S Roberts, G Castro, RP Dillon, A Kunz, H Kozachkov, MD Demetriou, WL Johnson, S Nutt, DC Hofmann “**Investigating Amorphous Metal Composite Architectures as Spacecraft Shielding**”, Adv Engrg Matls (2012)
DOI<<http://dx.doi.org/10.1002/adem.201200313>>



sound in the target). Subsequently, by increasing the hardness and density of the shield material, the minimum thickness of the shield to prevent a given amount of damage decreases. The density, diameter and velocity of the projectile also dramatically effect damage, but these parameters cannot be controlled during a real MMOD impact event. Lastly, the impact angle of the projectile affects the ballistic performance of a shield. A normal impact is expected to cause the most damage while a glancing (oblique) impact does the least damage. Although the trajectory of the projectile cannot be controlled, the design of the shield's surface morphology can affect the impact angle. Although BLEs are empirical for each material, trends in the performance of aluminum, titanium, and steel shields are useful for designing shields from new materials. For example, an optimal bumper shielding material which combines performance with overall cost is one that has an extremely high hardness and density with a multi-faceted facesheet (that turns a normal impact into an oblique one), while an optimal foam shield would have a cellular structure that diffuses the impact angle, disperses the debris cloud, and minimizes the shield system mass. While high hardness would imply that a ceramic shield would be optimal, their high melting temperatures prevent vaporization during MMOD impacts. Solid matter passing through the outer shield, as opposed to liquid and vapor, threatens the spacecraft wall. A truly optimal bumper material combines high hardness and low density with low-melting temperature, so that an MMOD impact vaporizes both the projectile and part of the shield.

Using these shield design criteria, amorphous metals (AMs) and AM-based metal-matrix-composites are strong candidates for bumper shielding. AMs are typically multicomponent alloys (usually consisting of three or more elements; titanium, zirconium, copper, aluminum, niobium,

beryllium, etc.) that are designed around deep eutectics, so as to have low-melting temperatures
Please cite this article as M Davidson, S Roberts, G Castro, RP Dillon, A Kunz, H Kozachkov, MD Demetriou, WL Johnson, S Nutt, DC Hofmann “**Investigating Amorphous Metal Composite Architectures as Spacecraft Shielding**”, Adv Engrg Matls (2012)
DOI<<http://dx.doi.org/10.1002/adem.201200313>>



(≈ 900 K) [14]. When cooled rapidly, crystallization of these alloys is avoided resulting in a random (amorphous) arrangement of atoms. When crystallization is sufficiently retarded, samples larger than 1 mm in thickness can be vitrified, creating bulk metallic glasses (BMGs) [15]. These alloys exhibit yield strengths near theoretical values (2 GPa), carbide-like hardness (650 Brinell, 60 Rc), processability similar to polymers, and large elastic limits (2%). However, single-phase BMGs typically lack toughness and ductility, so recent work has focused on developing BMG matrix composites reinforced with ductile-phase crystalline dendrites [16]. The resulting materials exhibit improved mechanical performance including tensile ductility (above 10%), ultra-high fracture toughness ($200 \text{ MPa m}^{1/2}$) and increased fatigue endurance limit (30% of yield strength) [17–20]. BMG composites are promising for use as bumper shields as they exhibit densities similar to titanium alloys ($5.1\text{--}5.8 \text{ g cm}^{-3}$ vs. $4.5\text{--}5.0 \text{ g cm}^{-3}$, respectively) but with more than twice the hardness (600 BNH vs. 250 BNH, respectively). The low-solidus temperatures and high viscosities of the BMG composites also enable unique panel fabrication methods. Semi-solid forging techniques have been developed previously to fabricate thin (<0.8 mm will thickness) panels of BMG composites in an “egg-box” configuration [21]. These panels, which exhibit alternating “up” and “down” pyramids, exhibit superior specific energy absorption values for cellular structures due to advantageous combinations of high strength, high ductility, and low-relative density. These structures also present a multi-faceted surface to an incoming projectile, ensuring that the impact angle is always near 45°. These combinations of features are investigated in the current study.

Thin panels of BMG composites were subjected to hypervelocity impacts at the NASA Ames Vertical Gun Range using a two-stage light gas gun capable of firing a variety of projectiles from a

Please cite this article as M Davidson, S Roberts, G Castro, RP Dillon, A Kunz, H Kozachkov, MD Demetriou, WL Johnson, S Nutt, DC Hofmann “**Investigating Amorphous Metal Composite Architectures as Spacecraft Shielding**”, Adv Engrg Matls (2012)
DOI<<http://dx.doi.org/10.1002/adem.201200313>>



sabot at velocities from 0.8 to 5.5 km s⁻¹, Figure 1a. BMG composite plates were fabricated by semi-solid forging [22]. The alloy was heated by induction to a temperature between the solidus and liquidus (≈ 1225 K), held isothermally to allow the microstructure to coarsen, and then forged using water-cooled copper molds, Figure 1b and d. DH1 (Zr_{36.6}Ti_{31.4}Nb₇Cu_{5.9}Be_{19.1}) BMG composite [17] was used in the forging of thin plates (0.5–1.0 mm thick) from 10 g ingots, Figure 1c, and thin egg-box panels (0.6 mm nominal wall thickness) from 25 g ingots, Figure 1e. The nominal microstructure from each alloy is shown in the inset of Figure 1e. The lighter contrast material is the coarsened dendrites and the darker material is the metallic glass matrix. The panels were fastened to a testing jig, Figure 1f, and impacted at a normal angle with velocities ranging from 0.8 to 3.0 km s⁻¹ using 3.17 mm aluminum spheres packed in a sabot. The charges were ignited using gunpowder and the sabot was stripped off directly after leaving the gun barrel. The velocity was measured using time-of-flight between sensors and the impact was captured using three laser-triggered cameras. Two cameras recorded each impact, a backlit one using 500 000 frames per second and another using 1 000 000, while a third was left with an open shutter to collect all the light emitted from the event. The setup is shown in Figure 1g.

Figure 2 shows two hypervelocity impacts from 3.17 mm spherical aluminum projectiles flying at 2.3 km s⁻¹ to contrast the performance of a BMG composite shield in different geometries (a thin plate and a multi-faceted egg-box). Six images captured in sequence during impact testing of the egg-box structure are exhibited in Figure 2a. The view is edge-on and backlit. The clamping screws are visible at the top and bottom of the sample. The impact occurred on a 45° angled surface of the egg-box and the event took ≈ 102 ms from the initial impact to the dissipation of the energy-release

flash. The links to the videos of Figure 2a and b can be found in the Supporting Information. Similar Please cite this article as M Davidson, S Roberts, G Castro, RP Dillon, A Kunz, H Kozachkov, MD Demetriou, WL Johnson, S Nutt, DC Hofmann “**Investigating Amorphous Metal Composite Architectures as Spacecraft Shielding**”, Adv Engrg Matls (2012) DOI<<http://dx.doi.org/10.1002/adem.201200313>>



impact conditions were used for a thin plate of the same BMG composite with approximately the same thickness, but in a flat configuration instead of the multi-faced one, and results are exhibited in Figure 2b. In comparison to the egg-box geometry, the flat plate has a much shorter energy-release flash and the debris cloud is much less diffuse as it travels down range. An estimation of the energy dissipated as light was obtained by counting the white pixels in each frame of video and plotting it versus the frame number, Figure 2c. The egg-box geometry produced a light intensity over four times greater than the flat plate when analyzing the data from the backlit camera and over 6.5 times greater when analyzing the non-backlit camera (which is set up to capture only light intensity). The number of illuminated pixels for the egg-box geometry was 537 781 and 915 049 using the backlit camera and the non-backlit camera, respectively, and the number of illuminated pixels for the flat plate geometry was 129 662 and 139 438, respectively. Moreover, the egg-box effectively diffused the debris cloud after the impact. Image analysis of at least 95% of the debris cloud was used to estimate the dispersion angle, Figure 2d and e. (The links to the videos of Figure 2d and e can be found in the Supporting Information.) The dispersion angle of the debris cloud was increased substantially by faceting the surface, from 76 to 1018 for flat and faceted surfaces, respectively. Figure 2f and g show a time-lapse image of the entire impact taken from a camera above the samples where all of the light generated in the image is from the impact (the red light is an LED that backlights the samples and pulses at the same frequency as the high-speed camera, 500 000 Hz). The single wall impact demonstrates the advantages of the thin, multi-faceted egg-box geometry to diffuse debris from the initial impact.

Please cite this article as M Davidson, S Roberts, G Castro, RP Dillon, A Kunz, H Kozachkov, MD Demetriou, WL Johnson, S Nutt, DC Hofmann “**Investigating Amorphous Metal Composite Architectures as Spacecraft Shielding**”, Adv Engrg Matls (2012)
DOI<<http://dx.doi.org/10.1002/adem.201200313>>

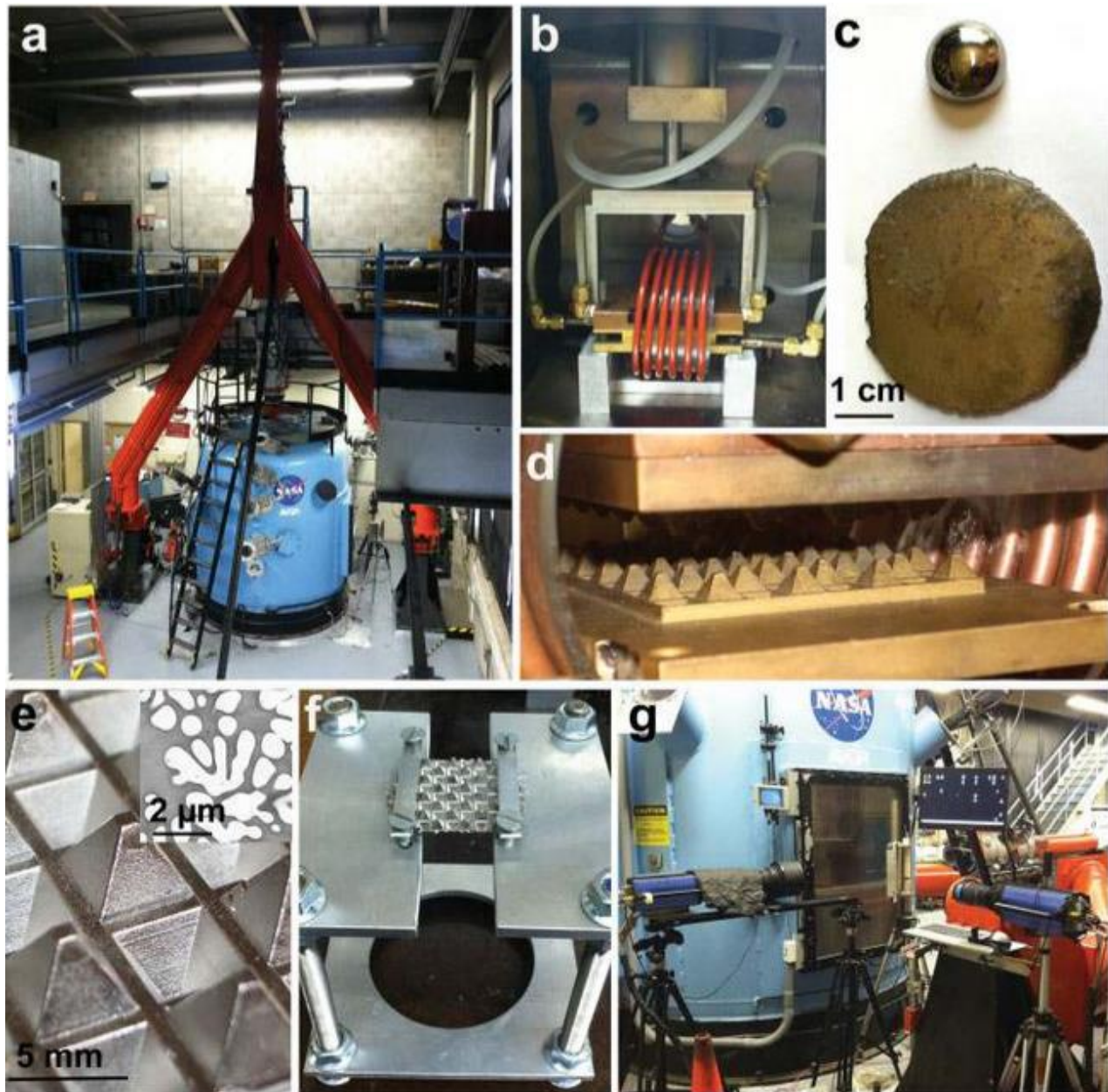


Figure 1: Hypervelocity facility and test samples – (a) View of the NASA Ames Vertical Gun Range which consists of a two-stage light gas gun capable of firing projectiles in two different configurations to allow simulations of impacts from 0.8 to 5.5 km s⁻¹. The environmental test chamber is over 2 m high and the angle of the impact can be changed using multiple ports on the side. (b) Forging chamber used to fabricate thin plates and egg-box structures. (c) Example of a 10 g ingot of the BMG composite DH1 (ZrTiNbCuBe) forged into a 0.8 mm thick sheet. (d) Mold used to forge egg-box panels from BMG composites. (e) BMG composite egg-box with a 0.6 mm thick wall fabricated using semi-solid forging technique and the nominal microstructure shown in the inset. (f) Egg-box panel fixed to testing jig. The hole in the bottom plate allows for the collection of debris from the impact. During some impacts, a witness plate was used instead to

Please cite this article as M Davidson, S Roberts, G Castro, RP Dillon, A Kunz, H Kozachkov, MD Demetriou, WL Johnson, S Nutt, DC Hofmann “**Investigating Amorphous Metal Composite Architectures as Spacecraft Shielding**”, Adv Engrg Matls (2012)
 DOI<<http://dx.doi.org/10.1002/adem.201200313>>



assess damage. (g) Setup of the high-speed cameras used to capture the impact. Three cameras can be seen in the image (one is at the upper right).

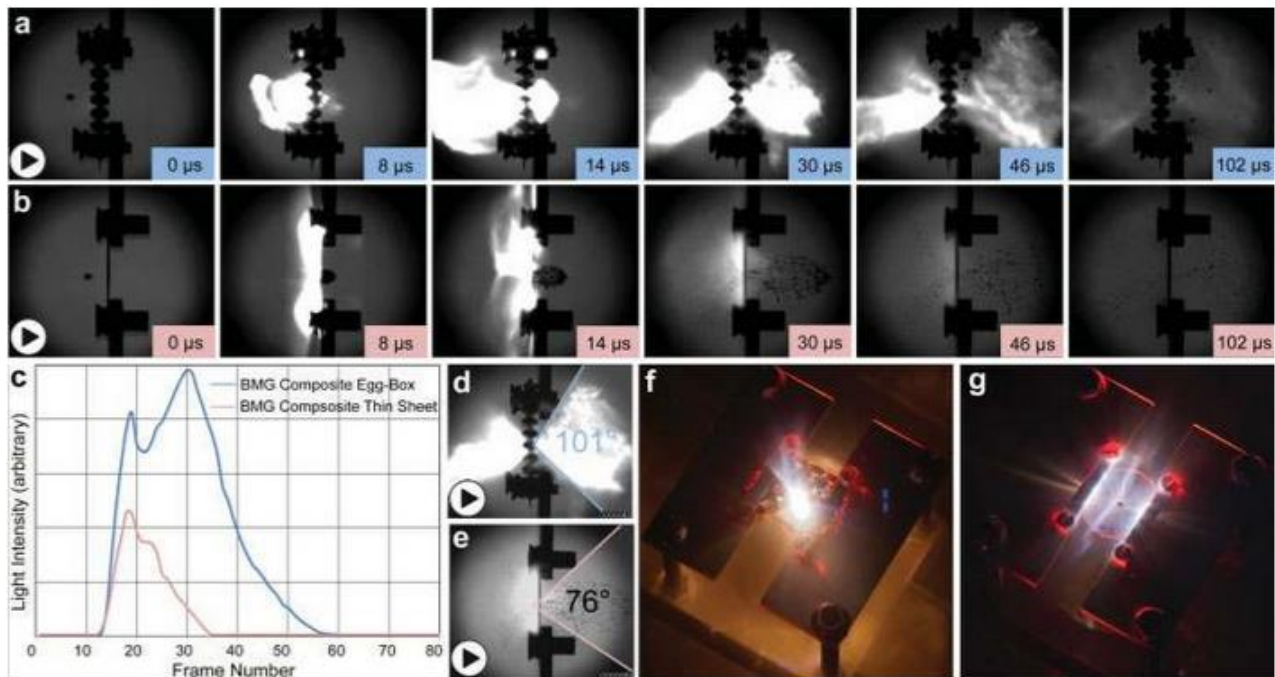


Figure 2: Comparison of surface geometry during hypervelocity impacts in BMG composite panels. (a) Backlit side-view images from a 3.17 mm aluminum sphere impacting a 0.6 mm thick ZrTiNbCuBe BMG composite egg-box, shown in (C), at 2.3 km s^{-1} for the first 102 ms after the impact. The multi-faceted surface effectively diffuses the impact into a broad debris cloud. The link to the video of Figure 2a can be found in the Supporting Information. (b) The same velocity impact as (a) into a 0.7 mm thick BMG composite sheet. The impact conditions and alloy are the same between (a) and (b) but the surface geometry is different. In (b) the debris cloud is tightly clustered after impact. The link to the video of Figure 2b can be found in the Supporting Information. (c) Plot of light intensity versus frame number for the hypervelocity tests in (a,b). As an estimation of energy released during impact, image analysis was used to determine the length and intensity of the light. The egg-box is much more effective than the thin sheet at dissipating energy. (d,e) Image analysis was used to designate a range of angle of the debris cloud that captures at least 95% of the debris. The egg-box geometry (d) has a 258 wider spread than the thin sheet (e). The links to the video of Figure 2d and e can be found in the Supporting Information. (f,g) Long exposure images from the impacts in the egg-box (f) and the thin sheet (g) illustrating the difference in light intensity during the impact. The red light is the laser used to trigger the high-speed cameras.

Cellular geometries have previously been employed for MMOD shielding. Specifically, aluminum HSPs have been used widely as spacecraft shielding due to their low-areal density and ability to diffuse MMOD impacts because of the cellular geometry [3,6,8–9]. HSPs are generally brazed to aluminum facesheets to form the shield, and their performance in hypervelocity tests is well-

Please cite this article as M Davidson, S Roberts, G Castro, RP Dillon, A Kunz, H Kozachkov, MD Demetriou, WL Johnson, S Nutt, DC Hofmann “**Investigating Amorphous Metal Composite Architectures as Spacecraft Shielding**”, Adv Engrg Matls (2012)
DOI<<http://dx.doi.org/10.1002/adem.201200313>>



established [3,6,8–9]. These shields exhibit drawbacks, however, including low hardness of the aluminum facesheets, a channeling effect during impacts caused by the honeycomb geometry that prevents dispersion of the debris cloud, low-intrinsic strength, and difficulties with brazing. A more effective metal cellular shield can be obtained by using a harder and higher strength metal and making the geometry stochastic (e.g., using random bubbles instead of tubular honeycombs). The challenge, however, is that these types of cellular structures are difficult to fabricate from conventional high-strength metal alloys, such as titanium and steel, due to the higher processing temperatures required to form them. Figure 3 demonstrates that BMG composite cellular structures can be fabricated simply by exploiting a unique property of the metallic glass matrix. Recently, it was demonstrated that BMGs exhibit a nearly constant electrical resistivity as a function of temperature (Johnson et al.[23]), and thus a capacitive discharge through a BMG rod results in rapid and uniform millisecond Ohmic heating. This technique was demonstrated by thermoplastically net-shaping BMG prototypes in 40 ms using rapid capacitive discharge. In this work, we employed the capacitive-discharge method to perform joining of BMG composites. In the current approach, the aim was not to achieve rapid uniform heating of the entire panels, but rather rapid uniform heating around the interfaces formed by the panels that are to be joined. This was achieved by discharging current from a capacitor using electrodes placed at the nodes of adjacent egg-box panels. As such, the glassy matrices of the BMG composite panels on each side of the interface are heated rapidly to a temperature between the solidus and liquidus temperatures bypassing crystallization and attaining a viscosity that is optimum for joining. Under such high heating rates the dendrite particulate does not have sufficient time for any transformation as the temperature traverses the undercooled liquid region (e.g., coarsening) or the semisolid region (e.g., melting). Consequently, the dendrite

Please cite this article as M Davidson, S Roberts, G Castro, RP Dillon, A Kunz, H Kozachkov, MD Demetriou, WL Johnson, S Nutt, DC Hofmann “**Investigating Amorphous Metal Composite Architectures as Spacecraft Shielding**”, Adv Engrg Matls (2012)
DOI<<http://dx.doi.org/10.1002/adem.201200313>>



morphology and thus the composite microstructure remain intact during this rapid joining process. By introducing two BMG parts between the electrodes, it is possible to localize that heating near the interface of the two components and by applying a compressive force during the capacitor discharge, the interface can be heated to a sufficient temperature to achieve a metallurgical bond, and then cooled rapidly to vitrify the BMG.

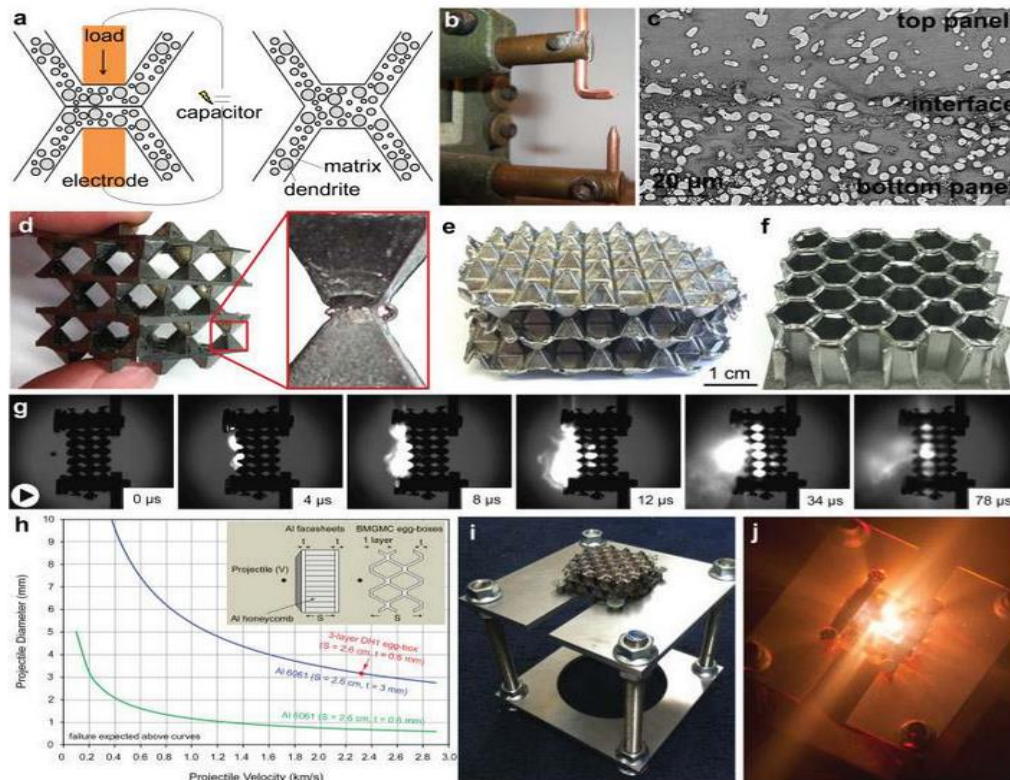


Figure 3: Hypervelocity impact in a welded BMG composite cellular structure. (a) Schematic of the capacitive joining process for a BMG composite. (b) Shaped electrodes on a spot welder were used to weld egg-boxes together. (c) SEM micrograph from two egg-box panels welded together. The interface is amorphous and the top and bottom panels exhibit a different nominal microstructure. (d) Image from a four-layer high BMG composite egg-box cellular structure obtained by capacitive welding the peaks of pyramids. The inset shows that the tips of each panel have been melted and fused together. The welded region cools rapidly enough to re-vitrify back into a glass, creating a high-strength joint. (e) The three-layer BMG composite cellular structure used for hypervelocity testing compared with an aluminum HSP structure (f) commonly used in space structures. (g) Backlit side view of the three layer egg-box structure being impacted by a 3.17 mm aluminum projectile at 2.3 km s^{-1} showing penetration of the first layer and slight penetration of the second layer. The link to the videos of Figure 3g can be found in the Supporting

Please cite this article as M Davidson, S Roberts, G Castro, RP Dillon, A Kunz, H Kozachkov, MD Demetriou, WL Johnson, S Nutt, DC Hofmann “**Investigating Amorphous Metal Composite Architectures as Spacecraft Shielding**”, Adv Engrg Matls (2012)
DOI<<http://dx.doi.org/10.1002/adem.201200313>>



Information. (h) Plot showing projectile diameter versus projectile velocity for aluminum sandwich panels with aluminum facesheets calculated from ballistic limit software. The green curve represents a HSP with the same thickness facesheets as the BMG composite egg-boxes and the same thickness as the three-layer welded egg-box structure. To achieve the same shielding capacity as the three-structure (shown in red), aluminum facesheets up to 3 mm thick must be used (blue curve). (i) The three-layer egg-box structure loaded into the sample holder and (j) a long exposure image showing the light generated during the impact.

A series of copper electrodes was designed with right-angled tips to weld the ends of the “down” pyramids of one panel with the “up” pyramids of another, Figure 3b. Using 60 J of discharge energy, the egg-box panels were welded at each joint to form a fully amorphous union, Figure 3c and d. Further details about this process, including the mechanical properties of the welded regions will be published elsewhere. Once two panels were welded at each joint, long projection-welding electrodes were used to weld on additional panels to form multi-layered structures (a four-layer BMG composite structure is shown in Figure 3d). Because of the unique capacitive joining capabilities of the BMG composites, $n \times n$ cellular structures are simple to fabricate, with no specialized equipment, brazing, or weakened heat-affected zone from welding. For hypervelocity testing, a three-layer thick cellular structure was constructed from BMG composites, Figure 3e, and clamped into a testing jig, Figure 3f. The similarities in the “cellular” nature of the three layer composite structure with an aluminum HSP is shown in Figure 3f. The top facesheet of the HSP was removed for viewing. In the HSP, impact debris is able to pass through the honeycomb structure easily, an effect called “channeling.” In the BMG composite egg-box structure, debris must perforate each multi-faceted layer of the egg-box to penetrate the structure. Hypervelocity testing was performed on the three-layer BMG composite egg-box by firing a 3.17 mm aluminum sphere at 2.3 km s^{-1} , as shown in Figure 3g, the link to the video of Figure 3g can be found in the Supporting Information. The projectile impacted an angled surface at 45°, similar to the single-layer test, and diffused between the first and second layer. The debris moved laterally in the fifth frame and then dissipated

Please cite this article as M Davidson, S Roberts, G Castro, RP Dillon, A Kunz, H Kozachkov, MD Demetriou, WL Johnson, S Nutt, DC Hofmann “**Investigating Amorphous Metal Composite Architectures as Spacecraft Shielding**”, Adv Engrg Matls (2012)
DOI<<http://dx.doi.org/10.1002/adem.201200313>>



out the top and bottom, and only a small region of detached spall reached the third layer. The welded joints remained intact throughout the impact and the kinetic energy of the projectile was mitigated. Figure 3h shows a plot of BLEs for aluminum HSPs provided by NASA's Johnson Space Center. The green curve represents an aluminum HSP with the same overall thickness as the three layered BMG structure (26 mm) and with facesheets equal in thickness to the wall of the BMG structure (0.6 mm). The performance of the three-layered BMG composite structure falls on the BLE for an aluminum HSP with thickness of 26 mm, but with much thicker facesheets (3 mm vs. 0.6 mm in the composite). Because the third layer of the BMG composite cellular structure was not perforated, the BLE for this structure lies above the blue curve in Figure 3e. Schematics of the two structures are shown in the inset of Figure 3h. The three-layer egg-box panel attached to the testing jig prior to impacting is shown in Figure 3i, and a long-exposure image of the entire impact is shown in Figure 3j. The present study involved a preliminary assessment of BMG composites as potential spacecraft shielding against the threat of MMOD. Utilizing known parameters obtained from hypervelocity testing of conventional (heritage) materials, BMG composite shield concepts were designed to exploit the critical material and geometric properties (mainly hardness, density, and impact angle) and tested using hypervelocity impacts. We demonstrated that welded panels of BMG composites offer a unique shielding solution for future satellites and spacecraft increasingly exposed to the threat of MMOD collisions. The current study was part of a larger joint effort between the Jet Propulsion Laboratory/California Institute of Technology and the University of Southern California to assess the performance of amorphous materials as spacecraft shields. As part of this broader effort, data was obtained for both monolithic metallic glasses and composites, including BLEs, penetration

Please cite this article as M Davidson, S Roberts, G Castro, RP Dillon, A Kunz, H Kozachkov, MD Demetriou, WL Johnson, S Nutt, DC Hofmann “**Investigating Amorphous Metal Composite Architectures as Spacecraft Shielding**”, Adv Engrg Matls (2012)
DOI<<http://dx.doi.org/10.1002/adem.201200313>>



depth, mass loss, multi-layer shield performance, spalling, and composite volume fraction. These results will be published in future work.

References:

1. Committee on Space Debris, National Research Council, Orbital Debris: A Technical Assessment, Nat. Acad. Press, Washington, D.C. 1995.
2. Scientific and Technical Subcommittee of the United Nations Committee on the Peaceful Uses of Outer Space, Technical Report on Space Debris, United Nations, New York 1999.
3. E. L. Christiansen, K. Nagy, D. M. Lear, T. G. Prior, *Acta Astronautica* 2009, 65, 921.
4. W. P. Schonberg, *Adv. Space Res.* 2010, 45, 709.
5. E. L. Christiansen, in: *Handbook for Designing MMOD Protection*, National Aeronautics and Space Administration Johnson Space Center, Houston, TX 2009, Ch. 1–4.
6. R. Destefanis, F. Schaefer, M. Lambert, M. Faraud, *Int. J. Impact Eng.* 2006, 33, 219.
7. S. Ryan, E. L. Christiansen, *Micrometeoroid and Orbital Debris (MMOD) Shield Ballistic Limit Analysis Program*. TM-2009-2147 89, National Aeronautics and Space Administration Johnson Space Center, Houston, TX 2010.
8. J. M. Sibeaud, L. Thame, C. Puillet, *Int. J. Impact Eng.* 2008, 35, 1799.
9. W. Schonberg, F. Schaefer, R. Putzar, *Acta Astronautica* 2010, 66, 455.
10. M. Grujicic, B. Pandurangan, C. L. Zhao, S. B. Biggers, D. R. Morgan, *Appl. Surf. Sci.* 2006, 252, 5035.
11. C. Yang, R. P. Liu, Z. J. Zhan, L. L. Sun, W. K. Wang, *Mater. Sci. Eng. A.* 2006, 426, 298.
12. C. J. Hayhurst, A. H. G. Livingstone, R. A. Clegg, R. Destefanis, M. Faraud, *Int. J. Impact Eng.* 2001, 26, 309.
13. C. Yang, W. K. Wang, R. P. Liu, L. Liu, X. Zhang, L. X. Li, *J. Spacecraft Rockets* 2006, 43, 565.
14. W. L. Johnson, *MRS Bull.* 1999, 24, 42.
15. A. Peker, W. L. Johnson, *Appl. Phys. Lett.* 1993, 63, 2342.
16. C. C. Hays, C. P. Kim, W. L. Johnson, *Phys. Rev. Lett.* 2000, 84, 2901.
17. D. C. Hofmann, J. Y. Suh, A. Wiest, G. Duan, M. L. Lind, M. D. Demetriou, W. L. Johnson, *Nature* 2008, 451, 1085.
18. D. C. Hofmann, J. Y. Suh, A. Wiest, M. L. Lind, M. D. Demetriou, W. L. Johnson, *Proc. Natl. Acad. Sci. USA* 2008, 105, 20136.
19. Y. Wu, Y. Xiao, G. Chen, C. T. Liu, Z. Lu, *Adv. Mater.* 2010, 22, 2270.
20. S. Pauly, S. Gorantla, G. Wang, U. Kuhn, J. Eckert, *Nat. Mater.* 2010, 9, 473.
21. J. P. Schramm, D. C. Hofmann, M. D. Demetriou, W. L. Johnson, *Appl. Phys. Lett.* 2010, 97, 241910.
22. D. C. Hofmann, H. Kozachkov, H. E. Khalifa, J. P. Schramm, M. D. Demetriou, K. S. Vecchio, W. L. Johnson, *JOM* 2009, 61, 11.
23. W. L. Johnson, G. Kaltenboeck, M. D. Demetriou, J. P. Schramm, X. Liu, K. Samwer, C. P. Kim, D. C. Hofmann, *Science* 2011, 332, 828.

Please cite this article as M Davidson, S Roberts, G Castro, RP Dillon, A Kunz, H Kozachkov, MD Demetriou, WL Johnson, S Nutt, DC Hofmann “**Investigating Amorphous Metal Composite Architectures as Spacecraft Shielding**”, *Adv Engrg Matls* (2012)
DOI<<http://dx.doi.org/10.1002/adem.201200313>>